Sustainable Food Technology

ROYAL SOCIETY OF CHEMISTRY

PAPER

View Article Online
View Journal | View Issue



Cite this: *Sustainable Food Technol.*, 2026, **4**, 1492

# Plant fibre-reinforced oilseed meal based biocomposites and biodegradable plates: development and performance analysis

Ruchi Rani, Prakash Verma, Sriram Marimuthu and Laxmikant S. Badwaik *

Received 3rd October 2025
Accepted 2nd December 2025

DOI: 10.1039/d5fb00647c

rsc.li/susfoodtech

The study addressed the challenge of developing minimally processed, flexible, and durable biodegradable plates using oilseed meals and plant fibres, a combination often limited by weak fibre–matrix bonding. Mustard, flaxseed, and soybean oilseed meals were blended with banana pseudostem, coconut coir, and sugarcane bagasse fibres, while emulsifiers, binders, cross-linkers, and plasticizers were incorporated to enhance compatibility. Biocomposites were fabricated using the solvent-casting method, and the plates were produced through hot compression moulding at 107 °C for 2 minutes. The biocomposites were characterized for mechanical, chemical, physical, and thermal properties, while the developed plates were evaluated for water-holding capacity, colour, contact angle, impact strength, spreadability, and biodegradability. The optimized plates exhibited moisture content of 7.28%, contact angle of 69.8°, water-holding capacity of 21.69%, fracturability of 144.54 N, and hardness of 155.96 N. Notably, the contact angle of the biodegradable plates was higher than that of the biocomposites, indicating improved surface hydrophobicity. Spreadability values were greater with water than with other food models. Biodegradability tests showed promising results, as decomposition began within 20 days, with residual plate weight reduced to approximately 35% of the original mass. These biodegradable plates can be converted to packaging trays which can be useful for storing fruits, eggs, mushrooms *etc.*

**Sustainability spotlight**

The development of biocomposites and biodegradable plates using agricultural by-products such as oilseed meals with plant fibres is a sustainable approach. Hot compression moulding was used for the development of biodegradable plates. The mechanical properties of plates suggest that they are suitable for single purpose biodegradable plates and decomposition begins within 20 days. This study attempts to reduce the constraints associated with the extraction of biomaterials from oilseed meals and plant fibres. The research work has market potential for boosting the economy of farmers as well as small scale industries and provides an opportunity to decrease the dependency on petroleum based plastics.

## 1. Introduction

Over the past several decades, consumerism has continually evolved, driving shifts in consumer preferences and accelerating the development of novel materials. In the current era, rising environmental awareness, the demand for lightweight and biodegradable alternatives, concerns over harmful emissions, and supportive governmental policies have collectively encouraged the pursuit of sustainable material solutions. Consequently, researchers and material developers are increasingly turning to nature-derived resources. In particular, many composite manufacturers are now prioritizing polymer matrices reinforced with plant-based natural fibers as promising eco-friendly options.[1] The best natural forms of biodegradable packaging and containers are found in seed shells and fruit rinds and peels. Biodegradability is an eco-friendly concept that benefits from both user and eco-friendliness. The processing of marine food and agricultural feedstocks generates a lot of waste by-products. Recycling these by-products can minimise pollution and maximise the preservation of natural resources while upholding safety and environmental friendliness. Biodegradable plastics are found in nursery pots used in agriculture, foam packaging for industrial items, and fast food flatware and food containers.[2] Moulded pulp products have been widely used in the disposable goods market because of its affordability, biodegradability, and ease of disposal. Moulded pulp products are replacing plastics in the food business as consumer expectations demand sustainable and eco-friendly products.[3] The market for single-use cutlery and tableware may be divided into product categories such as straws, chopsticks, glasses, spoons, forks, sporks, cups, and so on.[4]

*Department of Food Engineering and Technology, School of Engineering, Tezpur University, Napaam 784028, Assam, India. E-mail: laxmikantbadwaik@gmail.com; Fax: +91-03712-267005; Tel: +91-9706368117*

Usually, polymer, glass, and metal-based containers are commonly used for the purpose of rigid packaging in the food industry. Moreover, the use of wood pulp as biodegradable packaging has a primary disadvantage *i.e.* it consumes a massive amount of energy to create the cardboards.[5] However, hot compression, induction moulding, extrusion, solvent casting and hot mold baking procedures[6] are some of the common technologies used for the development of rigid containers such as trays, cutlery, *etc.* from plant fibres, fruit and vegetable wastes incorporated with polysaccharides, and they consume less energy for production. Oilseed meals are not commonly used in the area of rigid packaging.[2] Proteins that can be extracted from oilseed cake and utilised to create films with desirable properties, such as barrier and adhesive qualities and resistance to organic and oily solvents, are available at a reasonable cost.[7] The by-product of the widely used industrial process of extracting oil from sunflower seeds has intriguing qualities that make it suitable for injection moulding.[8] Many uses of proteins have been investigated, including their use as thermoplastics for non-food purposes. A thermoplastic polymer was initially made using oilseed meal. Oilseed crops such as soybean, mustard seed *etc.* are among the major industrial crops for the production of oil all over the world. After the extraction of oils from major oilseed sources, a substantial amount of de-oiled meals is produced, which is considered unfit for human or animal consumption due to the presence of anti-nutritional compounds.[9] With the increased use of plant oils as sustainable feedstocks, industrial oilseed meal can become a potential source for oilseed meal based biopolymeric films. The use of biopolymeric films and natural composite packaging materials with improved mechanical properties is demanded in a wider range of applications since most biopolymeric films have low mechanical properties in comparison to petroleum-based plastics.

Plants containing fibres of interest for the manufacture of engineering materials include coconut coir, sugarcane bagasse, banana pseudo-stem *etc.* The main advantages of using plant fibre are renewability, high strength and elastic modulus, low density, non-abrasiveness and biodegradability. There is a growing trend to use such fibres as fillers and/or reinforcers in plastic composites.[6,10–12] Scientists are working on the development of new packaging materials by treating fibres in various ways to increase their strength so that they can compete in the market with poly-oriented packaging materials, and their availability, quality and selection are influenced by geographic location.[13] The superior physico-mechanical properties of coconut fibers have led to increasing interest in their application as reinforcement in a wide variety of polymeric composites. Owing to their lignocellulosic nature, plant fibers have been successfully combined with thermoplastic matrices, which enables the fabrication of composite materials with improved mechanical strength and overall structural performance.[14] The field of moulded fibre technologies and products is experiencing rapid evolution. Interfacial bonding plays a crucial role in determining the overall properties of natural fiber composites, as effective stress transfer across the fiber–matrix interface is essential for improved reinforcement and restricted crack propagation. Challenges such as inadequate fiber wettability and moisture absorption, common to both natural fibers and certain polymer resins, further compromise composite performance. To address these issues, a variety of physical and chemical treatments have been employed to modify both fibers and matrices. Such modifications reduce moisture content, enhance compatibility, and strengthen the fiber–matrix interface, ultimately improving the stiffness, strength, and overall performance of natural fiber-reinforced polymer composites.[1] Cellulose is a moisture absorbent and exhibits hydrophilic behavior in plant fibers. Cellulose, the major component, is semicrystalline, whereas hemicellulose, which is partially soluble in water, is an amorphous polysaccharide. Lignin exhibits hydrophobic behavior and enhances the stiffness as a cementing agent. To fully realise the potential of moulded fibre products for a range of packaging applications, scientific knowledge and engineering design/practices are essential. The benefits of moulded fibre products include cost-effectiveness and environmental advantages. The food industry apps must comply with certain standards because of stringent guidelines.[3]

The present study aims to develop and characterize biocomposites and biodegradable plates by direct utilization of oilseed meals and plant fibres. The novelty of the study relies on the valorisation of agricultural by-products such as oilseed meals (mustard seed, flaxseed and soybean seed) and plant fibres (banana pseudo-stem, coconut coir and sugarcane bagasse). The research work has market potential for boosting the economy of farmers as well as small scale industries and will provide an opportunity to decrease the dependency on petroleum based plastics. It also paves the way for future research projects that will evaluate the unique functions and qualities of packaging.

## 2. Materials and methods

### 2.1. Materials

The plant fibres of banana pseudo-stem were collected from the campus of Tezpur University and the coconut coir, sugarcane bagasse, oilseed cakes (mustard, flaxseed and soybean seed) were collected from the vendors of Tezpur's local market, Assam. The chemicals and reagents used such as acacia gum, xanthan gum citric acid (m.w. 192.12 g $mol^{-1}$), glutaraldehyde (m.w. 100.12 g $mol^{-1}$), glycerol (m.w. 92.09 g $mol^{-1}$), *n*-hexane (m.w. 86.18 g $mol^{-1}$) and soy lecithin were procured from Hi Media Laboratories and Merck, India.

### 2.2. Methods

**2.2.1. Oilseed sample preparation.** The collected oilseed cakes were sorted manually, dried, and ground to powder form. The oilseed cake powder was sieved (150 mesh) and defatted with *n*-hexane (1 : 10 w/v) for 4 h. The defatted oilseed meals or powder were stored in a closed airtight container at 4 °C for further use.

### 2.3. Pre-treatment of plant fibres

The raw fibres were pre-treated with alkaline solution as shown in Fig. 1. The banana fibres (500 g) were cut into small pieces


Fig. 1 Extraction of fibres from (a) raw banana pseudo-stem, (b) raw coconut coir, and (c) raw sugarcane bagasse.

and were immersed into 6% NaOH (v/v) solution overnight at room temperature. After the alkali treatment, the fibres were easily separated and washed under running water until pH turned to neutral. The fibres were filtered and dried at 70 °C.[15] The coconut coir (200 g) was sorted and soaked in 10% (w/v) NaOH solution for 3 h in a 70 °C water bath with occasional stirring, followed by washing the fibres under running water multiple times to remove the soaked alkali until pH turned neutral. The fibres were dried at 70 °C.[16] The sugarcane bagasse (100 g) was immersed in 10% (w/v) NaOH alkaline solution for 1 h at room temperature under constant stirring. After the treatment, the fibres were sieved and washed with water until neutral pH was maintained and dried at 70 °C.[17] All the dried fibres were individually pulverized using a dry and wet pulverizer (Model: LP 20, Make: Lincon, India) to decrease the size of the fibres, sieved (52 mesh) and stored in airtight containers for functional, morphological, physicochemical and thermal property analysis.

### 2.4. Development of oilseed meal-gum crosslinked biocomposites incorporated with plant fibres

The composition of oilseed meals (mustard seed (20.50%) : flaxseed (67.15%) : soybean seed (12.33%)), natural gums (acacia & xanthan powder) (0.5 : 1.5% w/w) and crosslinkers (citric acid) (10% w/w) was optimized for development of biopolymeric films as per the report of Rani *et al.*[18] A similar composition was used for the development of biocomposites with addition of plant fibres of banana pseudo-stem, coconut coir and sugarcane bagasse at 1, 2, 3, 4 & 5% w/w of oilseed meals shown in Table 1.

Solvent casting was used to create biocomposites based on oilseed meals, natural gums and plant fibres. For the addition of the natural gums and crosslinkers, they were previously dissolved in 50 ml distilled water and heated at 80 °C for gelatinization on a magnetic stirrer at 900 rpm (ABDOS MS H280 Pro, India) for 15 min. Separately, the known quantity of the oilseed meals along with glycerol (75% w/w) as plasticiser is mixed separately in the remaining 50 ml distilled water on a magnetic stirrer at 900 rpm at 50 °C for 10 min. Afterwards, the natural gum crosslinker suspension is gradually added into the oilseed meal suspension with constant stirring at 900 rpm for uniform mixing for another 15 min at 50 °C. The entire mixture is heated to 90 °C for 30 min with occasional stirring, in a hot water bath (Modern, New Delhi), and then cooled in ice cold water. The suspension was mixed with 2% w/w soy lecithin, an emulsifier. Finally, the fibres of banana pseudo-stem, coconut coir and sugarcane bagasse with different percentages (1, 2, 3, 4 & 5% w/w) were incorporated into the final biocomposite suspension separately, and stirred for 15 min at 0 °C. The biocomposite suspension was poured into Petri plates after the air bubbles were removed by allowing the suspension to stand undisturbed for 10 minutes. To create uniform and smooth distribution, biocomposite Petri dishes (150 × 25 mm in size) were set using a portable spirit level and dried in a hot air oven at 70 °C for 72 h. Following drying, the biocomposites were carefully removed from the Petri plates, packed in ziplock pouches and

Table 1 Formulation for biocomposites and biodegradable plates incorporated with plant fibres

| Sl. no. | Oilseed meals[a] | Natural gums[b] | Crosslinker[c] | Banana pseudostem[d] (%) | Coconut coir[d] | Sugarcane bagasse fibre[d] (%) |
|---|---|---|---|---|---|---|
| 1 | Mustard seed meal (20.50%), | Acacia gum : xanthan gum | Citric acid (10% w/w of | 1 | 1 | 1 |
| 2 | flaxseed meal (67.15%), | (0.5 : 1.5% w/w of oilseed | oilseed meal) | 2 | 2 | 2 |
| 3 | soybean seed meal (12.33%) | meal) | | 3 | 3 | 3 |
| 4 | | | | 4 | 4 | 4 |
| 5 | | | | 5 | 5 | 5 |

[a] Ratios of oilseed meals from mustard, flaxseed and soybean were fixed as pre-determined in the study by Rani *et al.*[18] for all the composites. [b] The gum acacia and gum xanthan ratio of 0.5 : 1.5% (w/w) of the oilseed meal sample is constant for all the biocomposites. [c] Crosslinker (citric acid 10% w/w) represents the percentage addition of citric acid with respect to the total amount of oilseed meals in 100 ml of biocomposite suspension is constant for all the biocomposites. [d] BSF, CC & SBF (1–5%) represent the percentage addition of banana pseudostem, coconut coir & sugarcane bagasse fibre with respect to the total amount of oilseed meals in 100 ml of biocomposite suspension.

placed inside a desiccator containing dried silica gel for further examination.

### 2.5. Development of biodegradable plates incorporated with plant fibres

The formulation of the biodegradable plates included oilseed meal-gum and crosslinkers incorporated with plant fibres at 1, 2, 3, 4 & 5%, as presented in Table 1. To manufacture biodegradable plates, dough was prepared. For this, the mixture is prepared in 2 stages. First, a gel mixture was prepared with gums (acacia & xanthan), crosslinker (citric acid), plasticizer (glycerol 75% w/v) and emulsifier (soy lecithin 2% w/w) in 60 ml distilled water at 800 rpm (ABDOS MS H280 Pro, India) at 70 °C until mixed evenly. Then, the gel mixture is added to a dry mixture of oilseed meals and plant fibres (banana pseudo-stem, coconut coir and sugarcane bagasse).

The prepared dough is shaped into biodegradable plates using a hot compression moulding machine (MAZORIA, TCB-1 baking machine, India) as shown in Fig. 2. A circular double heat pan press coated with Teflon surfaces with a 208 mm diameter and a 9 mm thickness was used in the formation of biodegradable plates.[19] The machine was pre-heated for 2 min at 100 °C and greased with oil before use to avoid sticking. The homogeneous dough was formed and baked on a hot compression machine at 170 °C for 2 min to form sheets using manual hand pressing in such a way that the top pan mould was brought into contact with the bottom fixed pan and sealed tightly. After baking, the flattened baked sheets were removed from the machine. The final shape of the biodegradable plate was given by pressure moulding of the flattened baked sheets in between two structured plates for 10 min and removed slowly. Following moulding, the plates were dried for an additional 30 min at 102 °C in a hot air oven (IGene Labserve Model No. IG 95HA0) to eliminate any remaining moisture. It was then cooled in a desiccator before being placed in a low-density polyethylene (LDPE) bag for storage for further analysis.

### 2.6. Characterization of biocomposites

**2.6.1. Water solubility.** The biocomposite, measuring 2 cm by 2 cm, was dried at 105 °C and then immersed in 40 ml of distilled water, maintaining room temperature throughout the day with frequent stirring. Subsequently, the damp samples were extracted from the water and subsequently dried in a hot air oven at 105 °C for an additional 24 h.[20] Calculations were made on the sample's solubility using eqn (1).

$$\text{Total soluble matter (\%)} = \frac{(\text{initial dry weight} - \text{final dry weight})}{(\text{initial dry weight})} \times 100 \quad (1)$$

**2.6.2. Mechanical properties.** The textural and elongation properties were determined as per Badwaik *et al.*[21] using a texture analyser (TA-HD Plus Stable microsystems, UK). The texture analyser tension mode was pre-set at pre-test speed (5 mm $s^{-1}$), test speed (1 mm $s^{-1}$), and post-test speed (5 mm $s^{-1}$). The biocomposites were cut into 60 mm × 20 mm size pieces for measurement and placed in a grip with a load of 5 kg. The bio-composites were stretched upward until failure. Each biocomposite sample was run in triplicate. The maximum force and the distance between the grips on curves were recorded for

Fig. 2 Compression moulding machine.

further calculation of the tensile strength and the elongation at break.[22] The equations for the calculation of the mechanical properties are as given in eqn (2) and (3).

$$\text{Tensile strength (kPa)} = \frac{\text{maximum force of the film (N)}}{\text{cross sectional area of the film (m}^2\text{)}} \quad (2)$$

$$\text{Elongation at break (\%)} = \frac{\text{distance of rupture of film}}{\text{onset distance of the separation of film}} \times 100 \quad (3)$$

**2.6.3. Water vapor permeability.** The biocomposites were cut into 20 mm × 20 mm pieces, fixed and sealed in a glass beaker with round edges of diameter 50 mm partially filled with dried silica crystals (0% relative humidity). Then the sealed glass beaker with the biocomposite and silica was weighed and placed in a desiccator filled with saturated $K_2SO_4$ solution of relative humidity 97%, which was placed in an incubator set at 25 °C. The deviation in weight of biocomposites due to vapour exchange in the desiccator was recorded for 7 days every 24 h for the calculation of the water vapour transmission rate (WVTR). The slope of weight change as a function of time was calculated using linear regression (weight change *vs.* time), and the slope (g $h^{-1}$) divided by the biocomposite area gave the value of water vapour transmission rate.[23] The calculation of water vapour permeability was conducted using the following equation (eqn (4)).

$$\text{WVP (g Pa}^{-1}\text{ h}^{-1}\text{ m}^{-1}\text{)} = \frac{\text{WVTR}}{P(R1 - R2)} \times X \quad (4)$$

where $P$ = saturated vapor pressures of water (Pa) at room temperature, $R1$ = relative humidity of the desiccator with $K_2SO_4$ solution, $R2$ = relative humidity of the cup with dried silica crystals, $X$ = thickness of biocomposites (m) and the driving force under experimental conditions taken as $[P(R1 - R2)]$ is 3073.93 Pa.

**2.6.4. SEM.** The biocomposite's surface morphology was analyzed under a JSM 6390LV scanning electron microscope (JEOL, Japan). The thin layer of gold were coated on biocomposites and they were dried for 6 h at 60 °C and used for analysis.[23]

**2.6.5. DSC.** In order to investigate the thermal properties of the biocomposites, 0.01 g of the biocomposite sample was sealed in a pan and put into a differential scanning calorimetry (DSC) machine chamber. The biocomposite sample was heated at a rate of 10.0 K $min^{-1}$ from 20 °C to 300 °C using a Differential Scanning Calorimeter (214, Polyma, NETZSCH, Germany).[24]

**2.6.6. TGA.** TGA and DTG was performed using a TGA instrument (TG 209 F1 LIBRA, NETZSCH, Germany) to study the degradation characteristics of the biocomposites. The test was performed in the temperature range 25 °C to 600 °C with a heating rate of 10 °C $min^{-1}$ in nitrogen gas with 3–5 mg fibre samples.[25]

**2.6.7. XRD.** The material of the crystalline phase was identified through X-ray diffraction of the biocomposite sample, and cell dimensions were measured. An X-ray diffractometer (BRUKER AXS D8 FOCUS) was used to analyse the biocomposite. An X-ray beam operating at 100 mA and 50 kV was directed at the dried biocomposite sample. The area of the crystalline and amorphous regions was determined using the 2 theta curve, which ranges from 10 to 80°. The diffraction patterns were obtained using step scanning mode with $2\theta$ = 5–60°, 5 s per step, and a step of 0.02°.[26] The crystallinity degree was computed using eqn (5).

$$\text{Degree of crystallinity} = \frac{\text{area of crystalline peak}}{\text{total area under curve (crystalline + amorphous)}} \times 100 \quad (5)$$

**2.6.8. FTIR.** The biocomposites were subjected to infrared spectroscopy in order to determine the functional groups or chemical compounds contained inside. A Bruker Equinox 55 spectrometer (Bruker, Banner Lane, Coventry, UK) was used to evaluate the biocomposite pellets using Fourier transform infrared spectroscopy in the 400–4000 $cm^{-1}$ range.[27]

### 2.7. Characterization of biocomposites and biodegradable plates

**2.7.1. Moisture content and thickness.** The moisture content of biocomposites and biodegradable plates was determined by weight difference before and after drying in a hot air oven at 105 °C for 24 h until a constant weight was obtained as described in the report of Lee *et al.*[28] The thickness of the biocomposites and biodegradable plates was analysed using a micrometer at 3 random points (Alton M820–25, China) with a sensitivity of 0.01 mm.[29]

**2.7.2. Color.** The color parameters of the biocomposites and biodegradable plates were calculated using a Hunter Lab colorimeter (Ultrascan VIS, HunterLab, Inc., USA). The instrument was standardized using white and black tiles as lightness $L^*$ ($L^* = 0$ for black and $L^* = 100$ for white) and the color was recorded in reflectance of the sample. The recorded reading was analyzed in terms of chromaticity parameters $a^*$ (green [−] to red [+]) and $b^*$ (blue [−] to yellow [+]) [9]. The whiteness index (WI) was measured using eqn (6).[30]

$$\text{WI} = 100 - [(100 - L)^2 + a^2 + b^2]^{0.5} \quad (6)$$

**2.7.3. Contact angle.** The angle formed between the baseline of a droplet and the tangent line at the point where the water droplet makes contact with the surface is known as the contact angle. The hydrophilic or hydrophobic characteristic of the biocomposite surface can be determined by measuring the water contact angle.[31] The contact angle measurement was carried out using an Advanced Contact Angle Meter setup (Kyowa Interface Science VR, Japan). The biocomposites and biodegradable plates were cut into (2 cm × 2 cm) pieces, and using a syringe pump machine, the micro-droplets were created and then carefully placed on the cut samples. The subsequent water contact angles were calculated by the analysis of

 

photographs taken at various positions on biocomposite surfaces using a white light source and a high-speed camera.[32]

### 2.8. Characterization of biodegradable plates

**2.8.1. Mechanical properties.** The compression strength of the biodegradable plates was determined using a P-75 compression platen probe on a Texture Profile Analyser (TA-HD Plus, Stable Microsystems, UK). The biodegradable plates were turned upside down and the target strains of 10%, 30%, 50% and 70% were applied over the plates. The texture analyzer tension mode was set at a 5 mm $s^{-1}$ pre-test speed, 1 mm $s^{-1}$ test speed, 5 mm $s^{-1}$ post-test speed, and 1 N trigger force, also with a 100 kg load cell. The fracturability (N) and hardness (N) were determined from the graph plotting force (N) variations as a function of distance (mm).[5,33]

**2.8.2. Water holding capacity.** The biodegradable plates were cut into 2 cm × 2 cm size pieces and the initial weight ($W1$) of the sample was measured. Then, the samples were submerged in deionized water for a duration of 2 min. The final weight ($W2$) of the samples was weighed after removal of excess deionized water by filter paper from the surface of the sample.[5] The weight gained from water absorption was calculated using eqn (7).

$$\text{Water holding capacity } (\%) = \frac{(W2 - W1)}{W1} \times 100 \quad (7)$$

**2.8.3. Spreadability.** This test was performed according to method of Rana *et al.*[34] with little change to determine the maximum amount of time the biodegradable plates can brace water before outflow. It is a crucial way of determining plate performance in the presence of food. Five different food model (water, oil, syrup, honey and ketchup) variants were filled into the plates and checked every 5 min for leakage for 15 min at room temperature. The analysis was performed in triplicate.

**2.8.4. Biodegradability test.** The soil biodegradability test was analyzed as per the procedure of Changmai and Badwaik.[5] The biodegradable plates were cut, and the initial weight ($W1$) of the plate pieces was recorded. The sample pieces were then buried at a depth of 5 cm in pots filled with soil. The pots were incubated at room temperature for one month. The pot's soil was sprayed with water at regular intervals. The plate pieces were removed from the soil at 5 day intervals, washed, dried and their weight ($W2$) was noted. By tracking weight variations as a function of burial time, biodegradation was calculated. Lastly, using eqn (8), the weight loss of the container components was calculated.

$$\text{Weight loss } (\%) = \frac{(W1 - W2)}{W1} \times 100 \quad (8)$$

### 2.9. Statistical analysis

The biocomposites and biodegradable plates were examined using IBM SPSS Statistics 23 software. The mean differences of the biocomposites and biodegradable plates were compared using analysis of variance. The mean values of the biocomposite and biodegradable plate parameters were compared using Duncan's multiple range test ($p < 0.05$).

## 3. Results and discussion

### 3.1. Characterization of biocomposites added with plant fibres

**3.1.1. Thickness and moisture content.** The biocomposites incorporated with plant fibres had thickness ranging from 0.55 to 0.57 mm. Similar thickness was reported by Annandarajah *et al.*[35] and Singha *et al.*[27] Thickness is an important parameter to study the other beneficial properties of biocomposites such as mechanical and barrier properties, although maintaining the thickness made from natural sources for commercial use is still a challenge.[36] There was a significant difference ($p \leq 0.5$) between the values of thickness of biocomposites. The thickness of the biocomposites increased with addition in percentage of the fibres (Table 2). Physical and chemical treatment of natural fibers reduces the moisture content and enhances the bonding between the fiber and matrix. Therefore, the fibers and matrix together require modification in order to improve the interfacial adhesion, thereby resulting in enhanced strength and stiffness of natural fiber–polymer composites.

The moisture content of the biocomposites ranged from 30.74 to 31.38% in the banana fibre-added composite, 32.07 to 34.41% in the coconut coir-added composite and 24.82 to 32.18% in the sugarcane bagasse fibre added composite. The moisture content was found to be the highest in the 1% coconut coir added composite at 34.41% and was found to be the lowest in the 5% sugarcane bagasse fibre added composite at 24.82% (Table 2). The moisture content was reported to decrease with addition of plant fibres in the biocomposites. This decrease can be attributed to the hydrophobic nature of lignin present in the fibres.[37] A similar observation was made in the characterization of biopolymer films of alginate and babassu coconut mesocarp[35] and in sugarcane bagasse fibre on the properties of sweet lime peel and polyvinyl alcohol-based biodegradable films.[27] There was a significant difference ($p \leq 0.5$) found in the moisture content of the biocomposites.

**3.1.2. Water solubility.** The water solubility determines the weight loss and degradation process when the composite is disposed of in water and subjected to occasional agitation for a specific time. The water solubility (Table 2) of the composite with added plant fibres tends to increase significantly with addition in percentage of plant fibres.[27] The water solubility of the biocomposites was studied by keeping the composite in distilled water for 24 h. The solubility of the banana fibres added with biocomposites had solubility range 35.45 to 37.98%, whereas the biocomposites added with coconut coir and sugarcane bagasse fibres had solubility ranges 40.67 to 45.06% and 35.06 to 45.12%, respectively. The lowest solubility of 35.06% was found in the 1% sugarcane bagasse fibre added composite and the highest solubility of 45.12% was found in the composite added with 5% sugarcane bagasse fibres. The bound matrix particles start to be lost from fibres as they swell in high amounts of water. Addition of plant fibres increases the hydroxyl groups of nanocellulose, which increases the H bonding with water; thus, the proteins tend to solubilize in water.[38]

Table 2 Properties of biocomposites incorporated with plant fibres[a]

| Fibre biocomposites | Moisture content (%) | Thickness (mm) | Solubility (%) | Tensile strength (MPa) | Elongation at break (%) | Water vapor permeability $\times 10^{-10}$ (g $s^{-1}$ $m^{-1}$ $Pa^{-1}$) |
|---|---|---|---|---|---|---|
| OGCF 10% | 30.98 ± 1.00 | 0.55 ± 0.01 | 35.83 ± 0.37 | 1.15 ± 0.30 | 10.68 ± 0.83 | 3.8 ± 0.010 |
| Banana pseudostem 1% | 31.38 ± 0.18$^{de}$ | 0.55 ± 0.06$^{a}$ | 35.45 ± 0.21$^{a}$ | 1.17 ± 0.12$^{a}$ | 9.14 ± 0.43$^{abc}$ | 5.16 |
| Banana pseudostem 2% | 31.20 ± 0.26$^{cde}$ | 0.56 ± 0.03$^{b}$ | 36.18 ± 0.02$^{b}$ | 1.22 ± 0.19$^{ab}$ | 9.11 ± 2.74$^{bc}$ | 5.25 |
| Banana pseudostem 3% | 31.11 ± 0.35$^{cde}$ | 0.56 ± 0.03$^{b}$ | 37.68 ± 0.18$^{c}$ | 1.22 ± 0.39$^{ab}$ | 9.01 ± 1.38$^{abc}$ | 5.35 |
| Banana pseudostem 4% | 30.87 ± 0.26$^{cd}$ | 0.57 ± 0.03$^{c}$ | 37.31 ± 0.09$^{c}$ | 1.74 ± 0.33$^{b}$ | 7.51 ± 1.10$^{bc}$ | 5.69 |
| Banana pseudostem 5% | 30.74 ± 0.23$^{c}$ | 0.57 ± 0.04$^{c}$ | 37.98 ± 0.01$^{c}$ | 1.96 ± 0.0$^{a}$ | 7.11 ± 1.26$^{abc}$ | 6.25 |
| Coconut coir 1% | 34.41 ± 0.26$^{i}$ | 0.55 ± 0.04$^{a}$ | 40.67 ± 0.05$^{e}$ | 0.91 ± 0.23$^{a}$ | 9.69 ± 2.78$^{abc}$ | 4.88 |
| Coconut coir 2% | 33.73 ± 0.15$^{h}$ | 0.55 ± 0.03$^{a}$ | 43.55 ± 0.03$^{f}$ | 0.95 ± 0.13$^{a}$ | 7.14 ± 0.24$^{a}$ | 4.92 |
| Coconut coir 3% | 32.11 ± 0.22$^{fg}$ | 0.56 ± 0.03$^{b}$ | 44.22 ± 0.02$^{g}$ | 0.96 ± 0.26$^{a}$ | 7.09 ± 0.46$^{c}$ | 5.30 |
| Coconut coir 4% | 32.07 ± 0.32$^{fg}$ | 0.56 ± 0.05$^{b}$ | 44.95 ± 0.02$^{g}$ | 1.11 ± 0.36$^{a}$ | 6.89 ± 1.72$^{abc}$ | 5.36 |
| Coconut coir 5% | 32.07 ± 0.32$^{fg}$ | 0.57 ± 0.06$^{c}$ | 45.06 ± 0.02$^{h}$ | 1.30 ± 0.23$^{ab}$ | 5.61 ± 0.77$^{abc}$ | 5.37 |
| Sugarcane bagasse 1% | 32.18 ± 0.34$^{g}$ | 0.55 ± 0.02$^{a}$ | 35.06 ± 0.04$^{a}$ | 0.83 ± 0.12$^{a}$ | 8.89 ± 1.06$^{abc}$ | 4.55 |
| Sugarcane bagasse 2% | 31.62 ± 0.16$^{ef}$ | 0.56 ± 0.03$^{b}$ | 35.19 ± 0.02$^{a}$ | 0.91 ± 0.18$^{a}$ | 8.56 ± 0.94$^{abc}$ | 4.88 |
| Sugarcane bagasse 3% | 29.67 ± 0.17$^{b}$ | 0.57 ± 0.03$^{c}$ | 36.71 ± 0.02$^{b}$ | 1.12 ± 0.16$^{a}$ | 7.59 ± 1.96$^{abc}$ | 5.16 |
| Sugarcane bagasse 4% | 29.50 ± 0.19$^{b}$ | 0.57 ± 0.04$^{c}$ | 38.45 ± 0.03$^{d}$ | 1.15 ± 0.17$^{a}$ | 7.59 ± 0.96$^{ab}$ | 5.24 |
| Sugarcane bagasse 5% | 24.82 ± 0.17$^{a}$ | 0.57 ± 0.02$^{c}$ | 45.12 ± 0.21$^{h}$ | 1.28 ± 0.43$^{ab}$ | 6.19 ± 0.16$^{abc}$ | 5.56 |

[a] All the mentioned values are the mean of three replicates ± standard deviation. The letters superscripted as a–d on the values indicate significant differences ($p < 0.05$).

**3.1.3. Tensile strength.** The tensile strength determines the study of the mechanical properties of the biocomposites. The banana fibre (5%) added composite had the highest tensile strength of 1.74 MPa and the lowest tensile strength of 0.83 MPa was found in the 1% sugarcane bagasse fibre composite. The ranges of tensile strength for banana fibre, coconut coir and sugarcane bagasse composites were 1.17 to 1.96 MPa, 0.91 to 1.30 MPa and 0.83 to 1.28 MPa, respectively (Table 2). The tensile strength increased with the addition of plant fibres in the biocomposites. Although the composite appears brittle, it does not affect the mechanical strength of the composite. A similar observation was reported by Patel and Joshi,[39] who found that the tensile strength increased as the concentration of banana nanocellulose fibres increased, but further addition of nanofibres resulted in a decrease in tensile strength due to suspended nanoparticles making the composite brittle in texture. The primary chemical linkages occurring between the fiber and matrix in a biocomposite include covalent bonds and hydrogen bonds. These linkages, along with other forces, are crucial for effective stress transfer between the components and the overall performance of the composite material.

Previous researchers Jagadeesan *et al.*[40] found similar findings that addition of fillers more than 10%, due to lack of sufficient matrix to connect the matrix to the reinforcement, resulted in a reduction in tensile strength, and as the content of the reinforcement increased, the content of the matrix decreased for the development of sesame oil cake cellulose micro-fillers reinforced with a basalt/banana fibre-based hybrid polymeric composite.

**3.1.4. Elongation at break.** The mechanical property of elongation at break is analyzed using a texture analyser. This property is inversely proportional to tensile strength. The highest elongation at break was found in coconut coir reinforced biocomposites at 9.69% and the lowest percent elongation was found in 5% coconut coir reinforced biocomposites at 5.61%. The ranges of percent elongation for banana fibre, coconut coir and sugarcane bagasse composites were 7.11 to 9.14%, 5.61 to 9.69% and 6.19 to 8.89%, respectively. As seen in Table 2, as tensile strength of the biocomposites incorporated with plant fibres increases, the percentage elongation decreases.[41] A similar study was reported by Patel and Joshi,[39] where the addition of nanocellulose of banana plant fibres into polyvinyl alcohol to prepare a composite found that the tensile strength increases and then decreases as the composite becomes brittle. This exceptional result also affects the elongation of the composite as well portraying that though the strength of the biocomposites decreases with an increase in addition of nanocellulose, the elongation of the biocomposites increases and *vice versa*.

**3.1.5. Water vapor permeability.** The water vapor permeability gives the barrier property of biocomposites. The water vapor permeability was found to be the lowest in 1% sugarcane bagasse fibre reinforced composites at 4.55 g $s^{-1}$ $m^{-1}$ $Pa^{-1}$. The water vapor permeability was found to be the highest in the 5% banana fibre reinforced biocomposite at 6.25 g $s^{-1}$ $m^{-1}$ $Pa^{-1}$. The water vapor permeability ranges from 5.16 to 6.25 g $s^{-1}$ $m^{-1}$ $Pa^{-1}$, 4.88 to 5.37 g $s^{-1}$ $m^{-1}$ $Pa^{-1}$ and 4.55 to 5.56 g $s^{-1}$ $m^{-1}$ $Pa^{-1}$ for banana fibre, coconut coir and sugarcane bagasse fibre reinforced biocomposites (Table 2). The values of water vapor permeability increased with the addition of plant fibres in the composite. Also, the plant fibres such as banana pseudo-stem contain calcium crystals which develop micro-pores that elongate during the process of biocomposite drying and produce voids and gaps as observed in the morphological analysis in the biocomposites interrupting bonding of fibres in the matrix and prompt the exchange of gas and water vapors.[42] This similar behaviour was observed by Lopes *et al.*[36] when studying the water vapor permeability of composites formed by babassu coconut mesocarp, alginate and glycerol with 5.153 decreased to 3.615 g mm $m^{-2}$ $day^{-1}$ $kPa^{-1}$ after the second stage treatment of the films in aqueous $Ca^{2+}$ solution.

Table 3 Color and whiteness index of biocomposites incorporated with plant fibres[a]

| Fibres biocomposites | $L^*$ | $a^*$ | $b^*$ | WI |
|---|---|---|---|---|
| Banana pseudostem 1% | $27.06 \pm 0.17^{b}$ | $3.37 \pm 0.34^{cd}$ | $6.42 \pm 0.51^{c}$ | 22.50 |
| Banana pseudostem 2% | $27.03 \pm 3.17^{b}$ | $2.06 \pm 0.96^{abc}$ | $3.11 \pm 2.40^{ab}$ | 22.61 |
| Banana pseudostem 3% | $24.90 \pm 0.27^{ab}$ | $1.22 \pm 0.09$a | $1.22 \pm 0.05$a | 20.93 |
| Banana pseudostem 4% | $26.48 \pm 2.47^{ab}$ | $2.20 \pm 0.87^{abc}$ | $2.99 \pm 2.08^{ab}$ | 22.16 |
| Banana pseudostem 5% | $25.82 \pm 0.87^{ab}$ | $1.74 \pm 0.54^{ab}$ | $2.52 \pm 1.40^{ab}$ | 21.63 |
| Coconut coir 1% | $25.71 \pm 0.49^{ab}$ | $1.78 \pm 0.07^{ab}$ | $1.78 \pm 0.18^{ab}$ | 21.55 |
| Coconut coir 2% | $25.70 \pm 0.09^{ab}$ | $2.50 \pm 0.06^{abcd}$ | $2.08 \pm 0.26^{ab}$ | 21.53 |
| Coconut coir 3% | $25.37 \pm 0.07^{ab}$ | $2.03 \pm 0.34^{abc}$ | $1.93 \pm 0.32^{ab}$ | 21.28 |
| Coconut coir 4% | $25.13 \pm 0.07^{ab}$ | $2.83 \pm 0.69^{bcd}$ | $2.74 \pm 0.48^{ab}$ | 21.08 |
| Coconut coir 5% | $25.95 \pm 0.32^{ab}$ | $4.60 \pm 0.45^{e}$ | $4.12 \pm 1.39^{bc}$ | 21.65 |
| Sugarcane bagasse 1% | $26.24 \pm 2.59^{ab}$ | $2.71 \pm 0.98^{bcd}$ | $3.57 \pm 2.32^{ab}$ | 21.96 |
| Sugarcane bagasse 2% | $23.67 \pm 0.11$a | $1.74 \pm 0.25^{ab}$ | $1.71 \pm 0.16^{ab}$ | 19.98 |
| Sugarcane bagasse 3% | $24.64 \pm 0.25^{ab}$ | $2.57 \pm 0.06^{abcd}$ | $2.18 \pm 0.08^{ab}$ | 20.71 |
| Sugarcane bagasse 4% | $24.19 \pm 0.09^{ab}$ | $2.47 \pm 0.63^{abcd}$ | $2.35 \pm 0.29^{ab}$ | 20.37 |
| Sugarcane bagasse 5% | $24.58 \pm 0.27^{ab}$ | $3.64 \pm 0.69^{de}$ | $3.06 \pm 0.46^{ab}$ | 20.64 |

[a] All the mentioned values are the mean of three replicates ± standard deviation. The letters superscripted as a–d on the values show significant differences ($p < 0.05$).

**3.1.6. Color and whiteness index.** The color analysis and whiteness index of the biocomposites added with plant fibres were measured using a Hunter Lab colorimeter. The color analysis results of banana fibre, coconut coir and sugarcane bagasse fibre reinforced biocomposites were procured with respect to $L^*$, $a^*$ and $b^*$ and whiteness index. There was no significant difference found in the color of the coconut fibre added composite, but a significant difference ($p \leq 0.5$) was found in the banana fibre and coconut coir added composites as shown in Table 3. The $L^*$ values ranged from 24.90–27.06 for banana, 25.13–25.82 for coconut and 23.67–26.24 for sugarcane bagasse fibre added composites. All the values for $a^*$ and $b^*$ were found to be positive indicating the color of the composites was reddish yellow. The dark color of the composites was due to the raw agricultural materials of oilseed meals and plant fibres used as base for composite production.[43] The whiteness index was found to be the highest in 2% banana fibre added biocomposites at 22.61 and lowest in the 2% sugarcane bagasse fibre added composite (Table 3). The values of $L^*$, $a^*$ and $b^*$ were found to be the highest in 1% banana pseudostem biocomposites at 27.06, 5% coconut coir biocomposites at 4.60 and 1% banana fibre biocomposites at 6.42, respectively. The value of $L^*$ was found to be lowest in 2% sugarcane bagasse fibre biocomposites at 23.67 and the lowest value of $a^*$ and $b^*$ was found in 3% banana pseudostem biocomposites at 1.22 and 1.22, respectively. There were notable results of color analysis after addition of plant fibres at different concentrations, which influenced the color of biocomposites. The color of the composite gets darker as the concentration of plant fibres increases due to lignin and natural pigments in raw materials.[43,44] The $L^*$ values decrease from 27.06 to 24.90 in banana pseudostem based composites. A similar case was observed in the coconut coir and sugarcane bagasse fibre-based biocomposites.

**3.1.7. SEM.** Scanning electron microscopy was used to analyse the surface and cross section of the biocomposite reinforced with plant fibres. Fig. 3 shows the surface and cross-section of the banana pseudostem, coconut coir and sugarcane bagasse fibre based biocomposites. The addition of fibre strands is easily visible, dispersed on the surface of the composite.[45] As seen in SEM micrographs in case of the sugarcane bagasse fibre added composite, the surface of biocomposites is bound together within the biocomposites matrix, compactly layered with some roughness on the surface, indicating good dispersion.[26] The SEM micrographs show a bubble-free surface composite with the presence of visible plant fibre strings. After the chemical treatment of fibres with NaOH, the process of fibrillation occurs, which increases the active surface area available for contact of the waxy layer and intact lignocellulose components with the biocomposite matrix.[44,46,47] In the cross-section of the biocomposites, it was noticed that the fibre strand was pulled out of the film.[48] The composite also showed a rough surface, presence of voids *etc.*, and the voids in between the fibre and the matrix are due to improper cutting, tearing or presence of impurities.[46] Sugarcane bagasse added composites have smoother cross-section than coconut and banana fibre added biocomposites.

**3.1.8. XRD.** The crystal structures of the biocomposites were examined using X-ray diffraction (XRD). The XRD patterns of banana pseudostem, coconut coir and sugarcane bagasse fibre added composites are shown in Fig. 5. The percentage of crystallinity index of banana pseudostem fibre, coconut coir and sugarcane bagasse fibre added biocomposites was 34.02%, 43.88% and 46.38%, respectively. Fig. 4 shows the XRD of banana pseudo-stem, coconut coir and sugarcane bagasse fibres. We found that the major $2\theta$ diffraction peaks obtained in banana pseudo-stem fibers were at 22.26°, 15.55° & 35.18°. The major $2\theta$ diffraction peaks obtained for coconut coir were at 14.50°, 22.16° & 35.02°, whereas the major peaks obtained for sugarcane bagasse fibers were at 15.54°, 22.23° & 34.51°. But after the addition of fibres in the development of composites, there was a significant difference observed in the $2\theta$ diffraction peaks.

The main $2\theta$ diffraction peaks were recorded close to 14.97° and 22.4° for the banana pseudostem added composite; 34.97°, 22.16° and 14.61° for the coconut coir added composite;[49] and 15.58°, 22.23° and 34.55° for the sugarcane bagasse fibre added

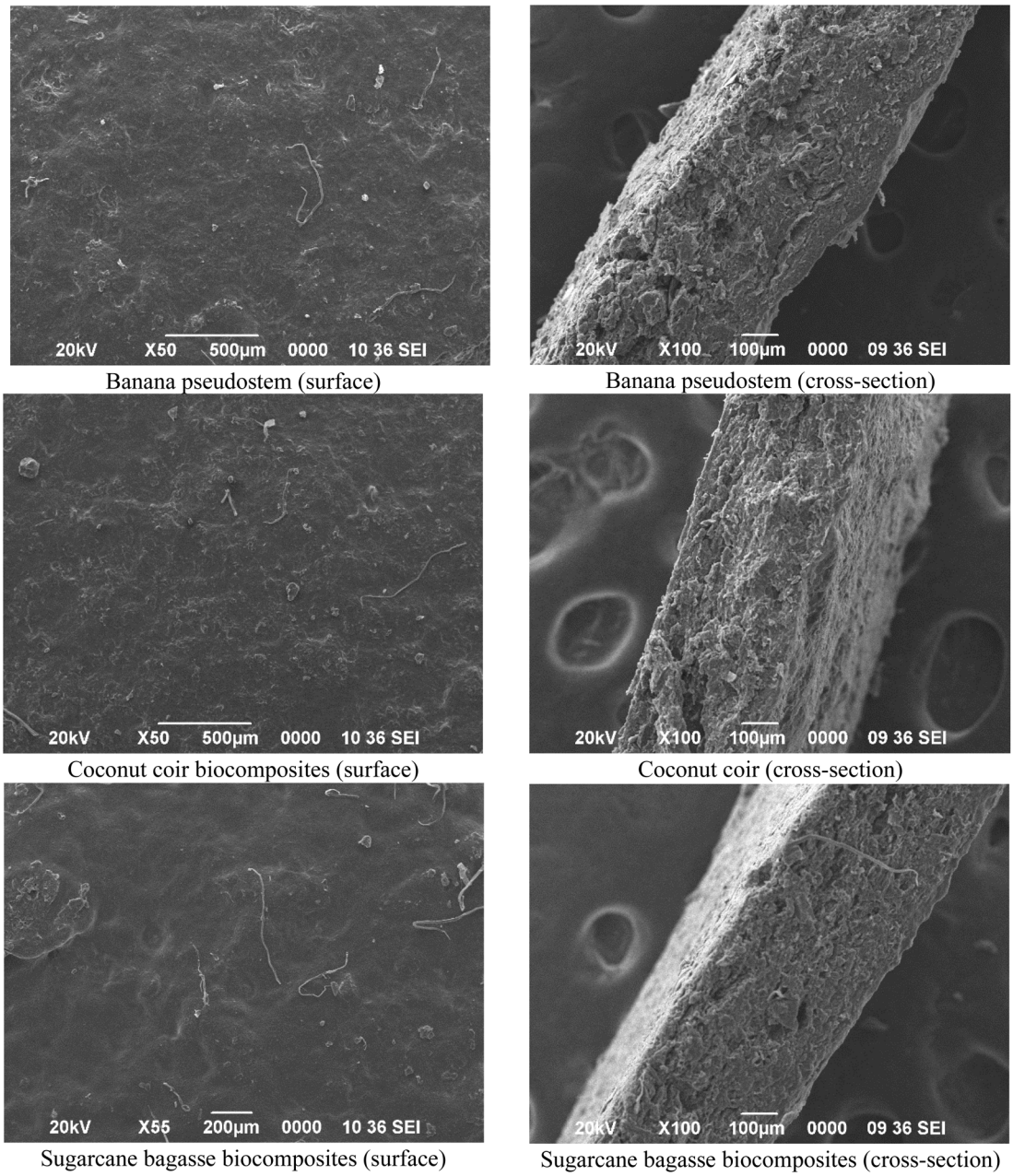


Fig. 3 SEM of biocomposites reinforced with plant fibres.

composite. A similar study was carried out by Shahi *et al.*[47] on cellulose film fabrication from sugarcane bagasse nanofibre extract. The 2$\theta$ diffractions were adjacent in the range of 16.5° to 22.2° and were associated with the presence of crystalline cellulose but sharp peaks were not observed in the graphs of XRD due to the partially amorphous nature[50] indicating that type I cellulose was converted into type II cellulose and many amorphous cellulose structures were generated during ionic liquid dissolution and regeneration.[51] The standard cellulose I structure, with crystalline peaks at 16.7°, 22°, and 34.08°, is present in all of the biocomposites. These peaks bear similarities to lignocellulosic source derivatives of cellulose.[40]

**3.1.9. TGA and DSC.** Thermogravimetric analyses are used to study the thermal stability and degradation process of the biocomposites over a wide temperature range. The TGA curves and DTG thermograms of the banana pseudostem, coconut coir and sugarcane bagasse fibre reinforced biocomposites are presented in Fig. 7. The TGA graph uses the DTG curve to determine the charts derivative of the sample attributed to time and temperature. The degradation of the sample such as mass loss, peak temperature and mass remaining after loss are recorded after the pyrolysis process of the biocomposites in the presence of nitrogen gas. The major mass loss was observed in 3 stages in all the biocomposites. In the 1st stage, mass loss for banana pseudostem, coconut coir and sugarcane bagasse fibre added composites was 7.34%, 9.13% and 9.98% at 31–197 °C, 47–196 °C and 37–189 °C, respectively, due to evaporation of extra bound moisture in the biocomposites. In the 2nd stage, mass loss for

 

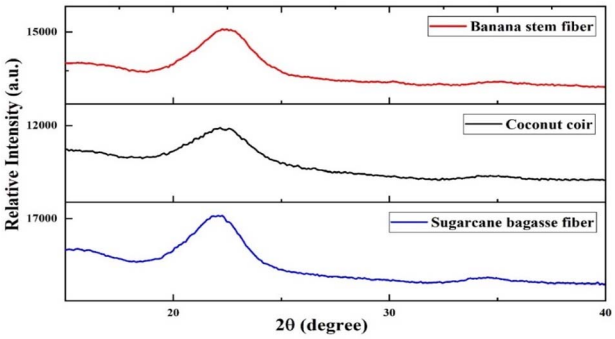


Fig. 4 XRD of (a) banana pseudo-stem, (b) coconut coir, and (c) sugarcane bagasse fibres.

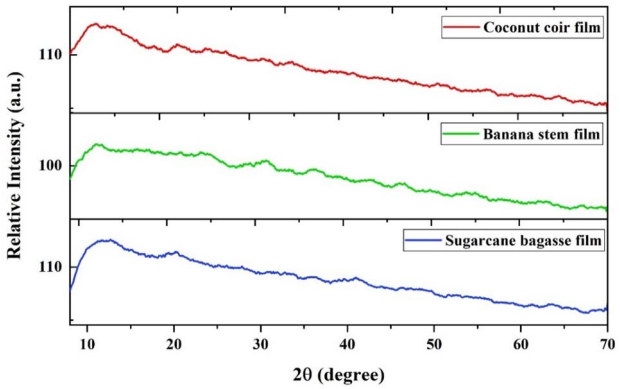


Fig. 5 XRD of biocomposites reinforced with plant fibres.

banana pseudostem, coconut coir and sugarcane bagasse fibre added composites was 41.9%, 42.64% and 38.18% at 197–342 °C, 196–343 °C and 189–346 °C, respectively. The wide range of mass loss is due to the decomposition of cellulose present in fibres in biocomposites. In the 3rd stage, mass loss for banana pseudostem, coconut coir and sugarcane bagasse fibre added composites was 11.35%, 13.97% and 10.08% at 342–598. °C, 343–597 °C and 346–597 °C, respectively. The higher temperature for decomposition was due to the degradation of non-cellulosic materials in the fibres and amount of lignin present in the fibres. The residual mass left after analysis was 29.55%, 29.71% and 28.24% for banana pseudostem, coconut coir and sugarcane bagasse fibre added composites, respectively.

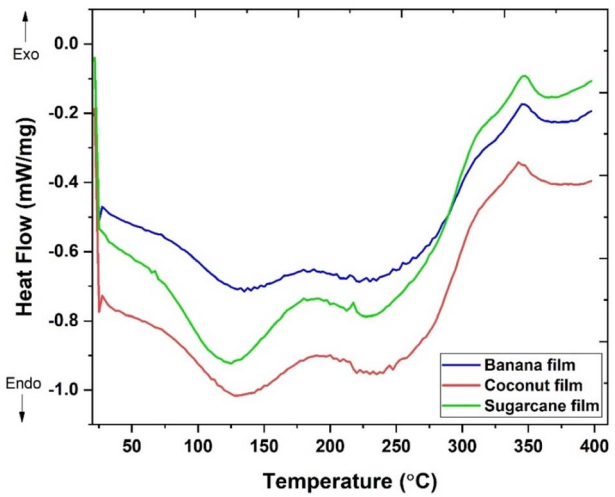


Fig. 6 DSC of biocomposites reinforced with plant fibres.

Table 4 presents the thermal properties of the biocomposites through DSC. DSC enables the study of different thermal parameters of the plant fibre enriched biocomposites such as melting temperature ($T_m$), crystallization temperature ($T_c$), glass transition temperature ($T_g$), and degradation temperature ($T_d$). As per the DSC thermographs obtained for the composites, there was presence of two endothermic peaks and one exothermic peak in all the graphs. The glass transition temperature ($T_g$) was obtained from the onset temperatures of the 1st endothermic peaks at 75 °C, 70 °C and 67 °C for banana pseudostem, coconut coir and sugarcane bagasse fibre added composites, respectively. According to DSC analysis in Fig. 6, it was reported that the first endothermic peak within the temperature range of 75 °C to 187 °C for banana fibre biocomposites, 70 °C to 197 °C for coconut coir biocomposites and 67–180 °C for sugarcane bagasse fibre biocomposites represents the downward shift of the temperature after incorporation of fibres into the biocomposite matrix showing the glass transition temperature of the biocomposites. The second endothermic peak within the temperature range of 187 °C to 285 °C, 197 °C to 277 °C and 180 °C to 280 °C represents the melting temperature of banana pseudostem, coconut coir and sugarcane bagasse fibre added biocomposites, respectively. The third and the last exothermic peak had a small temperature range from 325 °C to 372 °C, 315 °C to 370 °C and 315 to 365 °C for banana pseudostem, coconut coir and sugarcane bagasse fibre added biocomposites, respectively, representing degradation of the plant fibre's lignin presence in the biocomposites. The enthalpy of melting or fusion obtained for banana pseudostem added biocomposites was 6.58, 5.90 and 1.65 J $g^{-1}$ for the 1st and 2nd endothermic peaks and 3rd exothermic peak, respectively; the enthalpy of melting or fusion obtained for coconut coir added biocomposites was 50.65, 22.05 and 11.68 J $g^{-1}$ for the 1st and 2nd endothermic peaks and 3rd exothermic peak, respectively, and the enthalpy of melting or fusion obtained for sugarcane bagasse fibre added biocomposites was 13.96, 7.06 and 1.94 J $g^{-1}$ for the 1st and 2nd endothermic peaks and 3rd exothermic peak, respectively.[40,41,52–54]

**3.1.10. FTIR.** Functional groups can be used to determine the chemical structure of any treatment.[38] The FTIR spectra of the banana pseudostem, coconut coir and sugarcane bagasse fibre reinforced biocomposites are presented in Fig. 8. The common band recorded in all the biocomposites was in the wavenumber range of 3427–3432 $cm^{-1}$ for the OH stretching alcohol intermolecular bond of cellulose. The band in the wavenumber range 2900–2922 $cm^{-1}$ indicated the presence of chlorophyll and that at 2800–3000 $cm^{-1}$ was attributed to N–H stretching of amine salt. The band in the 2851–2854 $cm^{-1}$ wavenumber range in the graph represents the possibility of aldehydes in the biocomposites. There was presence of strong

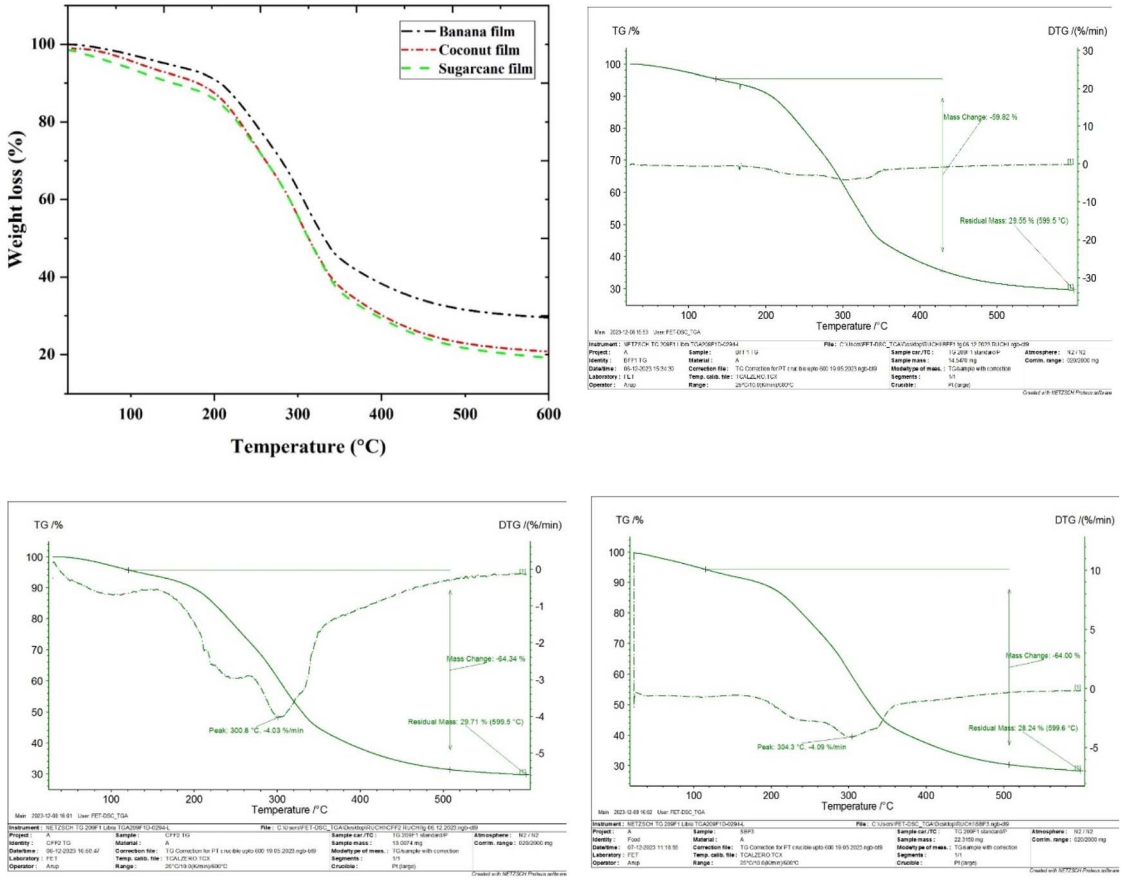


Fig. 7 TGA of biocomposites reinforced with plant fibres.

C=O stretching and OH bending of moisture in the form of water-soluble hemicellulose in the range 1733–1715 $cm^{-1}$. In the wavenumber range 1735–1738 $cm^{-1}$, there was a band attributed to the α,β-unsaturated ester of carboxylic stretching group of ferulic acid. The presence of cellulose symmetric deformation of the $CH_2$ group noted at 2364 $cm^{-1}$ and 2330 $cm^{-1}$ was due to the presence of hemicellulose attributed to OH stretching of the carbonyl group. The presence of hemicellulose in the biocomposites was clearly shown in the wavenumber range 1249–1731 $cm^{-1}$. The band at 1648–1658 $cm^{-1}$ indicated the presence of C=C stretching vibration of alkene vinylidene. The strong stretching of the nitro-compound in the range between 1550 and 1500 $cm^{-1}$ and at 1409 $cm^{-1}$ shows the presence of sulfonyl chloride. Both the nitro-compound and sulfonyl chloride show the presence of oilseed meals in the biocomposites. The peak at 1443 $cm^{-1}$ is attributed to the C–O–C bond of the cellulose chain. The presence of skeleton vibration of lignin in the biocomposites was observed by C–H asymmetric deformation, medium O–H alcohol bending, absorption associated with stretching vibrations of aromatic

Table 4 DSC of biocomposites incorporated with plant fibres

| | Banana pseudostem added biocomposites | | | Coconut coir fibre added biocomposites | | | Sugarcane bagasse fibre added biocomposites | | |
|---|---|---|---|---|---|---|---|---|---|
| | Melting temperature range (°C) | | Enthalpy ($J\ g^{-1}$) | Melting temperature range (°C) | | Enthalpy ($J\ g^{-1}$) | Melting temperature range (°C) | | Enthalpy ($J\ g^{-1}$) |
| Peaks | $T_o$ | $T_e$ | $\Delta H_m$ | $T_o$ | $T_e$ | $\Delta H_m$ | $T_o$ | $T_e$ | $\Delta H_m$ |
| 1st endotherm | 75 | 187 | 6.58 | 70 | 197 | 50.65 | 67 | 180 | 13.96 |
| 2nd endotherm | 187 | 285 | 5.90 | 197 | 277 | 22.05 | 180 | 280 | 7.06 |
| 3rd exotherm | 325 | 327 | 1.65 | 315 | 370 | 11.68 | 315 | 365 | 1.94 |

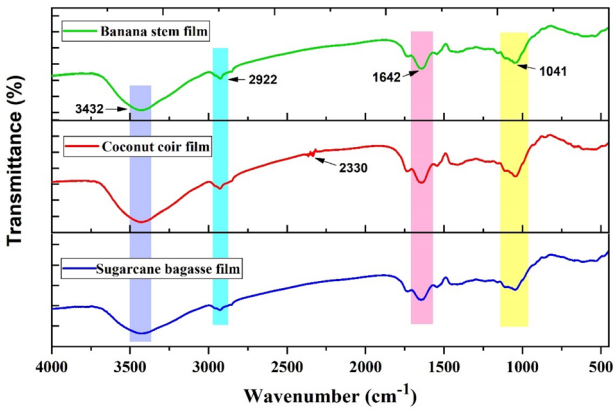


Fig. 8 FTIR of biocomposite reinforced with plant fibres.

C=C and acetyl group of hemicellulose recorded at wavenumbers 1313–1378 $cm^{-1}$. In the wavenumber range of 1230–1245 $cm^{-1}$ was the presence of lignin skeleton stretching of C–O. In the range 1150–1087 $cm^{-1}$, data showed strong C–O stretching of an aliphatic ether and in the range 1040–1060 $cm^{-1}$ the strong broad band attributed to CO–O–CO stretching of anhydride and glycosidic linkages was observed, indicating high content. At wavenumbers between 1030 and 1070 $cm^{-1}$, strong S=O sulfoxide stretching due to the presence of oilseed meals was observed. The symmetric in-phase stretching mode in lignin at 674 $cm^{-1}$ and at 525 $cm^{-1}$ showed a narrow peak associated with in-plane aromatic ring deformation vibration common for carbon presence.[16,47–49,55,56]

### 3.2. Characterization of biodegradable plates

To order to achieve the best combination of plant fibres to be used for the development of biodegradable plates, the plant fibre reinforced biocomposites were primarily developed and analysed. Through the analysis based on mechanical, barrier, physical and thermal properties, it was determined that the ideal percentage for biocomposite formulation was 5% of plant fibres (banana pseudo-stem, coconut coir and sugarcane bagasse). The developed biodegradable plates were further analyzed on the basis of physical, mechanical, color and biodegradability.

The average thickness of the banana pseudo-stem fibre added biodegradable plates was 4.45 mm; that of coconut coir fibre added biodegradable plates was 4.72 mm; and that of sugarcane bagasse fibre added biodegradable plates was 4.07 mm. The study is found to be similar to the result reported by Changmai and Badwaik,[5] and Ferreira *et al.*[57] The thickness of the biodegradable plates is shown in Table 5.

The $L^*$, $a^*$ and $b^*$ of banana pseudo-stem, coconut coir fibre and sugarcane bagasse fibre added biodegradable plates was 31.10, 32.73, and 30.26; 9.16, 9.63, and 8.79; and 13.66, 15.13, and 12.57, respectively. The color analysis results are presented in Table 5. This darkness in color of the biodegradable plates was due to the dark color of the oilseed meals as raw materials and the fibres (banana pseudo-stem, coconut coir and sugarcane bagasse) added in the development of plates also impart brown color of lignin.[6]

**3.2.1. Moisture content.** The moisture content of the biodegradable plates is shown in Table 5. The moisture content of banana pseudo-stem fibre added biodegradable plates was 11.58%; that of coconut coir fibre added biodegradable plates was 7.28%; and that of sugarcane bagasse fibre added biodegradable plates was 11.68%. Less than 10% (wb) moisture content produced a stiffer, stronger sample. Higher moisture levels in the samples make them less stiff, perhaps insufficient to hold the weight of the desired product, and so less useful.[2] Similar findings were observed in the report of Harkrishnan *et al.*[58] where the cutlery product developed from virgin coconut oil cake and wheat bran fibre had 12.29% moisture content and that developed from virgin coconut oil cake with gaur gum had 12.30% moisture content.

**3.2.2. True density.** A substance's true density is determined by dividing its compressed mass by its volume without air. Finding the actual density of each component in a composite material, such as plant fibres, is crucial when choosing a material, particularly if a lightweight composite is required.[59] The true density of the biodegradable plates is presented in Table 5. The true density was found to be the highest in banana pseudo-stem fibre at 0.73 g $cm^{-3}$ in comparison to those of coconut coir fibre (0.66 g $cm^{-3}$) and sugarcane bagasse fibre (0.57 g $cm^{-3}$) added biodegradable plates. The density was found to be higher than that of biodegradable foam trays developed with cassava starch blended with the natural polymers of kraft fibre and chitosan whose density is 0.14 g $cm^{-3}$.[6]

**3.2.3. Contact angle.** The micro-texture and its adhesion play an important role in the study of contact angle. The surface

Table 5 Physical properties and color analysis of biodegradable plates incorporated with plant fibres[a]

| Properties | BPBS | BPCC | BPSB |
|---|---|---|---|
| Moisture content (%) | $11.58 \pm 0.13^{b}$ | $7.28 \pm 0.21^{a}$ | $11.68 \pm 0.20^{b}$ |
| Thickness (mm) | $4.45 \pm 0.32^{a}$ | $4.72 \pm 0.21^{a}$ | $4.07 \pm 0.50^{a}$ |
| Water holding capacity (%) | $26.89 \pm 1.59^{ab}$ | $29.82 \pm 3.03^{b}$ | $21.69 \pm 2.44^{a}$ |
| True density | $0.73 \pm 0.02^{c}$ | $0.66 \pm 0.01^{b}$ | $0.57 \pm 0.02^{a}$ |
| $L^*$ | $31.10 \pm 2.26^{ab}$ | $32.73 \pm 1.31^{b}$ | $30.26 \pm 1.24^{a}$ |
| $a^*$ | $9.16 \pm 0.50^{a}$ | $9.63 \pm 0.42^{a}$ | $8.79 \pm 0.77^{a}$ |
| $b^*$ | $13.66 \pm 1.10^{ab}$ | $15.13 \pm 0.80^{b}$ | $12.57 \pm 1.14^{a}$ |

[a] BPBS = biodegradable plates added with banana pseudo-stem fibres, BPCC = biodegradable plates added with coconut coir fibres & BPSB = biodegradable plates added with sugarcane bagasse fibres. All the mentioned values are the mean of three replicates ± standard deviation. The letters superscripted as a–d on the values show significant differences ($p < 0.05$).

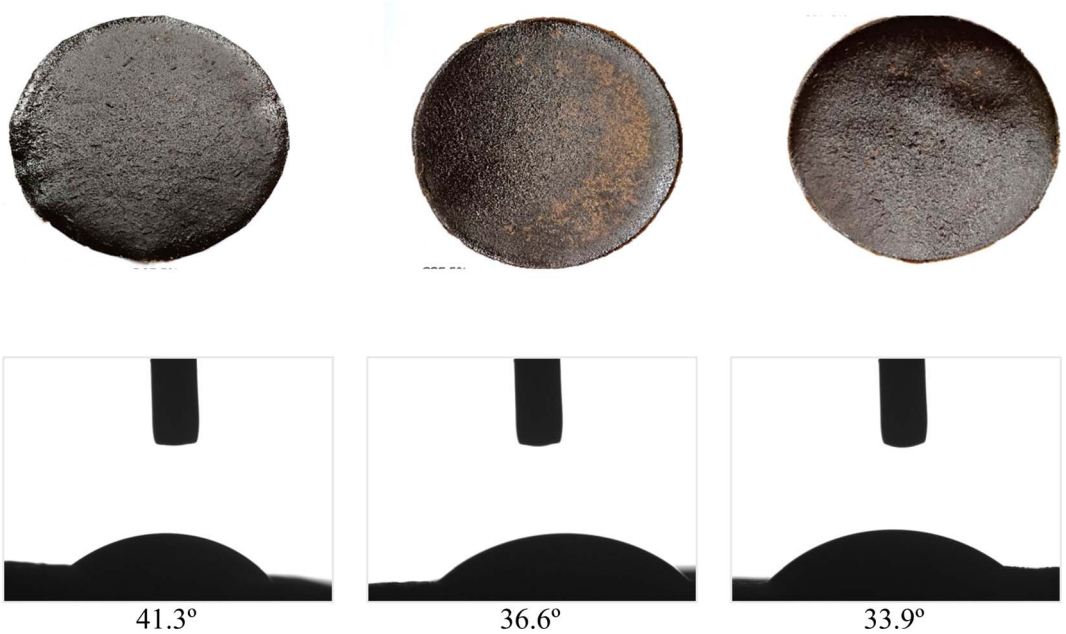


Fig. 9 Contact angle of biocomposites reinforced with plant fibres.

with water contact angle >150° has low adhesion and the water drop tends to roll off even at low tilting angle of the base, whereas the surface with water contact angles <150° have high adhesiveness and have anisotropic wetting properties with distinct water angles. That means, higher the contact angle, higher is the water hydrophobicity.[32] The contact angle of the biocomposites is presented in Fig. 9 and the contact angle of the biodegradable plates is presented in Fig. 10. The contact angles of biocomposites incorporated with banana pseudo-stem, coconut coir and sugarcane bagasse fibres were 41.3°, 36.6° and 33.9°, respectively. The contact angle was found to be the highest for banana pseudo-stem fibre added biodegradable plates at 69.8° compared to that of coconut coir fibre added biodegradable plates at 42.8°, while sugarcane bagasse fibre added biodegradable plates had a 49.3° contact angle. The contact angle of biodegradable plates was found to be higher than that of biocomposites. There is an inverse relationship between a material's contact angle and wettability. The contact angle was found to be lower than that of pure bee wax (97°) and bee wax modified with 15% zinc stearate used for coating the surface of sweet lime pomace-based containers with polyvinyl alcohol, starch sodium and carboxy methyl cellulose.[5] The lower

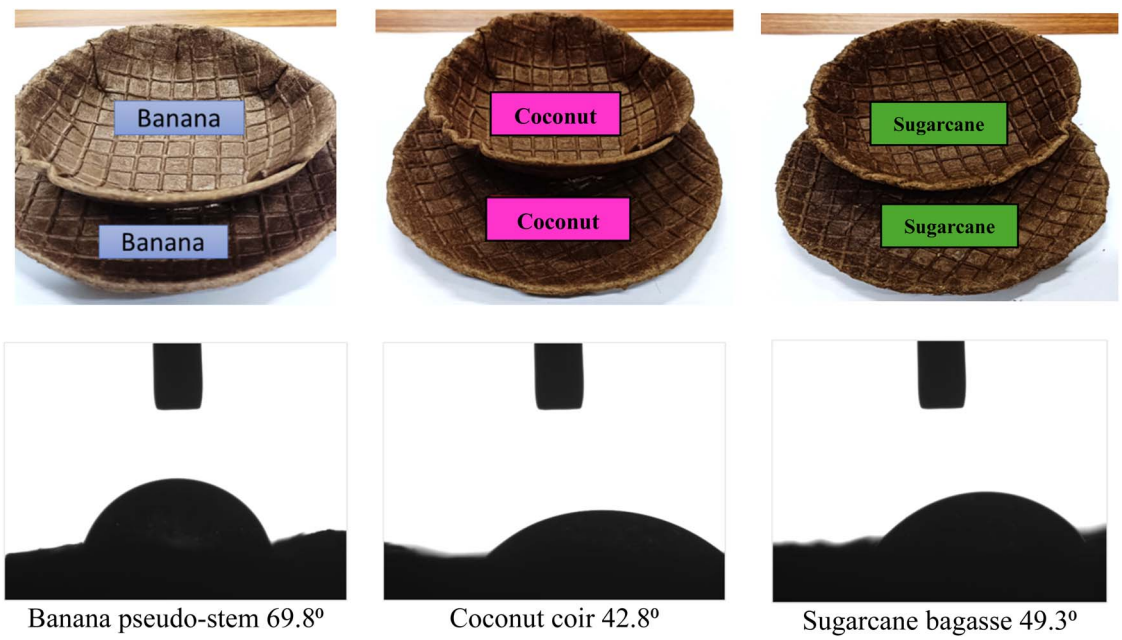


Fig. 10 Contact angle of biodegradable plates incorporated with plant fibres.

 

Table 6 Compression test (%) of the biodegradable plates[a]

| Biodegradable plates | Percent compression (%) | Fracturability (N) | Hardness (N) |
|---|---|---|---|
| BPBS | 10 | 37.58 ± 0.02 | 84.28 ± 1.11 |
| | 30 | 82.71 ± 0.01 | 84.82 ± 0.02 |
| | 50 | 95.06 ± 0.07 | 97.80 ± 0.03 |
| | 70 | 103.02 ± 0.02 | 114.80 ± 0.08 |
| BPCC | 10 | 33.71 ± 0.00 | 40.05 ± 0.09 |
| | 30 | 34.81 ± 0.03 | 61.58 ± 0.02 |
| | 50 | 68.75 ± 0.01 | 108.53 ± 0.01 |
| | 70 | 144.54 ± 0.05 | 155.96 ± 1.51 |
| BPSB | 10 | 47.35 ± 0.07 | 76.02 ± 1.31 |
| | 30 | 67.94 ± 1.14 | 105.36 ± 0.07 |
| | 50 | 67.65 ± 0.06 | 144.03 ± 0.03 |
| | 70 | 129.25 ± 0.03 | 145.93 ± 0.04 |

[a] BPBS = biodegradable plates added with banana pseudo-stem fibres, BPCC = biodegradable plates added with coconut coir fibres & BPSB = biodegradable plates added with sugarcane bagasse fibres.


Fig. 11 Spreadability test of the biodegradable plates with different food models within 15 min.

contact angle in the biodegradable plates can be due to high porosity and uneven texture without any coating on the plates.

**3.2.4. Water holding capacity.** The water holding capacity or water absorption capacity of banana pseudo-stem fibre added biodegradable plates was 26.89%, that of coconut coir fibre added biodegradable plates was 29.82%, and that of sugarcane bagasse fibre added biodegradable plates was 21.69%. A similar water absorption capacity increase was noted in edible cutlery spoons developed by employing wheat flour, ragi flour, sorghum flour and Indian ginseng root powder from 9.70% to 39.50% within 30 min.[33] The water holding capacity of the biodegradable plates is presented in Table 5.

**3.2.5. Hardness and fracturability.** The mechanical properties like hardness and fracturability were studied by a compression test (at 10%, 30%, 50% and 70%) strains for the biodegradable plates. Biodegradable plates are generally hard and unbendable in structure unlike other disposable plastic and paper plates. Therefore, there was a need to test the strength and force needed to break the biodegradable plates.[34] The values obtained for hardness and fracturability of the biodegradable plates are reported in Table 6. At 10% strain, the sugarcane bagasse had the highest fracturability value of (47.35 N) compared to banana pseudostem (37.58 N) and coconut coir (33.71 N) fibre based biodegradable plates whereas at 70% strain, coconut coir based biodegradable plates had the highest value of fracturability of (144.54 N) compared to sugarcane bagasse (129.25 N) and banana pseudostem (103.02 N) fibre based biodegradable plates. The hardness value at 10% strain was found to be the highest in banana pseudostem (84.28 N) compared to sugarcane bagasse (76.02 N) and coconut coir (40.05 N) whereas at 70% strain, the hardness required to break the plates was found to be the highest in coconut coir (155.96 N) compared to sugarcane bagasse (144.03 N) and banana pseudostem (114.80 N) fibre based biodegradable plates. There were similar findings showing that with the addition of binder and increasing the amount of fibre in the raw material

Table 7 Absorption capacity of the biodegradable plates with different food models within 15 min[a]

| Biodegradable plates | Absorption capacity (%) |
|---|---|
| BPBS (oil) | 1.86 ± 0.68 |
| BPCC (oil) | 1.44 ± 0.08 |
| BPSB (oil) | 1.57 ± 0.48 |
| BPBS (honey) | 1.43 ± 0.15 |
| BPCC (honey) | 1.50 ± 0.08 |
| BPSB (honey) | 0.88 ± 0.10 |
| BPBS (ketchup) | 1.61 ± 0.22 |
| BPCC (ketchup) | 1.53 ± 0.42 |
| BPSB (ketchup) | 1.69 ± 0.16 |
| BPBS (syrup) | 1.26 ± 0.06 |
| BPCC (syrup) | 1.87 ± 0.38 |
| BPSB (syrup) | 0.79 ± 0.13 |
| BPBS (water) | 3.24 ± 0.08 |
| BPCC (water) | 3.88 ± 1.83 |
| BPSB (water) | 3.36 ± 0.33 |

[a] BPBS = biodegradable plates added with banana pseudo-stem fibres, BPCC = biodegradable plates added with coconut coir fibres & BPSB = biodegradable plates added with sugarcane bagasse fibres.

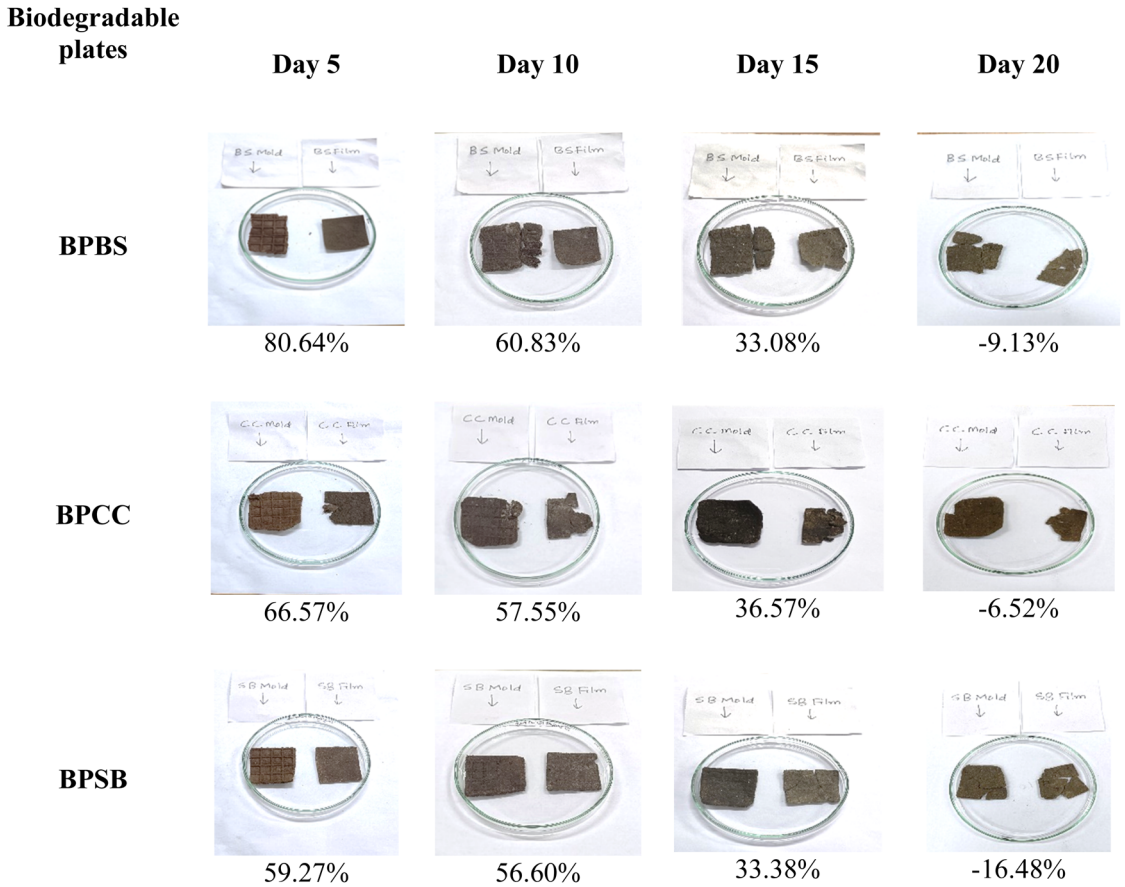


Fig. 12 Biodegradability test of biodegradable plates reinforced with plant fibres. The values presented below each image are the leftover weight percentage.

increased the samples' tensile strength. Biodegradable plates should have a higher tensile strength.[58]

**3.2.6. Spreadability test.** A test was performed to analyse the withholding capacity of water or different fluids in the biodegradable plates until the specified time at room temperature.[34] All the plates were subjected to different food samples including water for 15 min and their results were recorded. There was no leakage, but the water was observed to spread and got absorbed more quickly than syrup when placed in all three biodegradable plates added with banana pseudo-stem, coconut coir and sugarcane bagasse fibres within 15 min, whereas there was no spreadability observed in the plates in the presence of oil, honey or ketchup. Also, the rate of absorption was very low in the presence of oil, honey or ketchup in comparison to water within 15 min. As presented in Fig. 9, coconut fiber reinforced biodegradable plates had a lower contact angle than sugarcane bagasse and higher contact angle than banana pseudostem at 42.8°, 49.3° and 69.8°. This shows that coconut coir added biodegradable plates had the highest water absorption capacity and all the plates exhibit hydrophilic properties. The data recorded related to the spreadability test and absorption capacity are presented in Fig. 11 and Table 7, respectively.

**3.2.7. Biodegradability test.** The process *via* which a polymer is broken down by microorganisms into biomass, carbon dioxide, water, or methane is known as biodegradation.[60] The samples were placed in the soil and humidity of the soil was maintained and the results were analysed. Each sample was weighed every 5 days. The values of sample weight recorded were found to decrease as shown in Fig. 12. As per images, the biodegradable plates were recorded to decompose within 20 days. Since the plates are developed from biodegradable ingredients, they started swelling and decomposing the following day and decomposed within 30 days as they gradually broke down into tiny pieces. The swelling was also seen when the plate samples were taken out from the soil, similarly to what was reported by Hazra and Sontakke,[33] and Rodrigues *et al.*[61] The weight of the sample gradually decreased due to the action of enzymes released by microorganisms involved in abiotic decomposition.[61,62] The biodegradation was found to be the highest in the sugarcane bagasse incorporated plates in comparison to the banana pseudo-stem and coconut coir incorporated plates. The plates were photographed in triplicate every 5 days as presented in Fig. 12.

## 4. Conclusions

Developing a market for industrial uses provides farmers with diversified income streams, which can actually help stabilize the agricultural sector and encourage the cultivation of a wider range of crops, ensuring overall agricultural resilience. The composites

and biodegradable plates made with oilseed meals reinforced with plant fibers can replace non-biodegradable, petroleum-based plastics with bio-based alternatives; the practice contributes to environmental sustainability. The products can benefit us with their various applications within the food industry and in other sectors as well. They are easy to prepare, need less energy in comparison to other commercially available products and are non-toxic and eco-friendly in nature. Plant fibre (5%) addition was found to be the most suitable concentration for producing compactable and structurally stable biocomposites for biodegradable plate formation. This enables manufacturers to standardize fibre loading to achieve consistent mechanical performance in bio-tableware production. The addition of plant fibres decreased moisture content and elongation at break, while increasing thickness, tensile strength, water vapor permeability, and water solubility. All of this enhances the functional strength of disposable plates, making them suitable for serving dry and semi-moist foods. Morphological analysis revealed uniform roughness, indicating that effective dispersion of plant fibres within the matrix ensures better bonding and structural integrity, beneficial for manufacturing sturdy, crack-resistant food packaging items. Fibre incorporation increased thermal stability and percent crystallinity of the biocomposites making the plates more heat-resistant, thus allowing their use for warm food items and enhancing suitability for industrial thermoforming processes. FTIR analysis verified the presence of polysaccharides, proteins, chlorophyll, and other fibre components, confirming successful biomaterial integration. The functional property supports the development of biodegradable products with predictable degradation behaviour, useful for eco-friendly packaging industries. The resulting plates were rigid, showed improved contact angle compared to biocomposites, and exhibited acceptable food-grade properties. This enables direct use in commercial food service operations, replacing single-use plastic plates. The study confirmed that plant fibres are compatible with oilseed meal matrices, improving composite formation and reducing processing limitations, facilitating the utilization of agricultural by-products in value-added bio-based materials, supporting circular bioeconomy models. The streamlined development approach minimizes the need for intensive extraction of biomaterials from fibre and meal sources and thus decreases manufacturing cost and processing time, making bio-tableware more accessible for small-scale industries. The research demonstrates potential to boost farmer income, support small enterprises, and reduce dependence on petroleum-based plastics. The research also promotes sustainable rural development, encourages biodegradable packaging sectors, and contributes to national plastic-waste reduction initiatives.

## Ethical statement

This study does not involve any human or animal testing.

## Author contributions

Ruchi Rani: data curation, methodology, formal analysis, investigation; writing-original draft; Prakash Verma: formal analysis, investigation; Sriram Marimuthu: formal analysis, investigation; Laxmikant S. Badwaik: conceptualization, project administration, resources, supervision, writing-review & editing.

## Conflicts of interest

The authors have declared that there is no conflict of interest for this work.

## Data availability

All data are presented in this article.

## Acknowledgements

Authors are thankful for the support received from DST-FIST and UGC-SAP for carrying out the work.

## References

1 A. Ramachandran, S. M. Rangappa, V. Kushvaha, A. Khan, S. Seingchin and H. N. Dhakal, *Macromol. Rapid Commun.*, 2022, **43**(17), 2100862.
2 E. Mohareb and G. S. Mittal, *Packag. Technol. Sci.*, 2007, **20**(1), 1–15.
3 Y. Zhang, C. Duan, S. K. Bokka, Z. He and Y. Ni, *J. Bioresour. Bioprod.*, 2022, **7**(1), 14–25.
4 K. Dybka-Stępień, H. Antolak, M. Kmiotek, D. Piechota and A. Koziróg, *Polymers*, 2021, **13**(20), 3606.
5 N. J. Changmai, L. S. Badwaik and J. Packag, *Technol. Res.*, 2021, **5**(2), 107–114.
6 N. Kaisangsri, O. Kerdchoechuen and N. Laohakunjit, *Ind. Crops Prod.*, 2012, **37**(1), 542–546.
7 S. Popović, N. Hromiš, D. Šuput, S. Bulut, R. Romanić and V. Lazić, in *Cold Pressed Oils*, Academic Press, 2020, pp. 15–30.
8 A. Rouilly, O. Orliac, F. Silvestre and L. Rigal, *Bioresour. Technol.*, 2006, **97**(4), 553–561.
9 S. Kaza, L. Yao, P. Bhada-Tata and F. Van Woerden, *What a Waste 2.0: A Global Snapshot of Solid Waste Management to 2050*, World Bank Publications, 2018.
10 S. S. Teh, A. E. D. Bekhit, A. Carne and J. Birch, *Journal of Food Measurement and Characterization*, 2014, **8**, 92–104.
11 M. R. Koushki, M. H. Azizi, M. Azizkhani and P. Koohy-Kamaly, *J. Food Qual. Hazards Control*, 2015, **2**(2), 45–50.
12 N. Mohan, S. Natarajan and S. P. Kumaresh Babu, *J. Miner. Mater. Charact. Eng.*, 2010, **9**(3), 231.
13 F. Muneer, E. Johansson, M. S. Hedenqvist, M. Gällstedt and W. R. Newson, *BioResources*, 2014, **9**(3), 5246–5261.
14 D. Behera, S. S. Pattnaik, D. Nanda, P. P. Mishra, S. Manna and A. K. Behera, *Emergent Mater.*, 2025, **8**(1), 157–172.
15 T. Hariprasad, G. Dharmalingam and P. P. Raj, *J. Mech. Eng. Sci.*, 2013, **4**, 518–531.
16 M. D. F. Rosa, E. Medeiros, J. A. Malmonge, K. S. Gregorski, D. F. Wood, L. H. C. Mattoso, G. Glenn, W. J. Orts and S. H. Imam, *Carbohydr. Polym.*, 2010, **81**(1), 83–92.

17 A. R. Bertoti, S. Luporini and M. C. A. Esperidião, *Carbohydr. Polym.*, 2009, **77**(1), 20–24.
18 R. Rani, T. Gosh and L. S. Badwaik, *Sustainable Chem. Pharm.*, 2023, **33**, 101147.
19 S. Marimuthu, A. Saikumar and L. S. Badwaik, *Biomass Convers. Biorefin.*, 2025, **15**(5), 7763–7777.
20 S. M. Ojagh, M. Rezaei, S. H. Razavi and S. M. H. Hosseini, *Food Chem.*, 2010, **122**(1), 161–166.
21 L. S. Badwaik, P. K. Borah and S. C. Deka, *Carbohydr. Polym.*, 2014, **103**, 213–220.
22 R. Rani and L. S. Badwaik, *Int. J. Biol. Macromol.*, 2024, **265**, 130809.
23 B. Deepa, E. Abraham, L. A. Pothan, N. Cordeiro, M. Faria and S. Thomas, *Materials*, 2016, **9**(1), 50.
24 S. Zhang, N. Kim, W. Yokoyama and Y. Kim, *Food Chem.*, 2018, **243**, 202–207.
25 R. K. Gond, M. K. Gupta and M. Jawaid, *Polym. Compos.*, 2021, **42**(10), 5400–5412.
26 M. Yumnam, D. Hatiboruah, R. Mishra, K. Sathyaseelan, P. Nath and P. Mishra, *Sens. Actuators, A*, 2023, **361**, 114557.
27 P. Singha, R. Rani and L. S. Badwaik, *Sustainable Food Technol.*, 2023, **1**(4), 610–620.
28 J. Lee, R. Durst and R. Wrolstad, in *Official Methods of Analysis of AOAC International*, AOAC International, 2005, Method 2005.02.
29 F. M. Pelissari, F. Yamashita, M. A. Garcia, M. N. Martino, N. E. Zaritzky and M. V. E. Grossmann, *J. Food Eng.*, 2012, **108**(2), 262–267.
30 J. H. Lee, H. J. Yang, K. Y. Lee and K. B. Song, *Int. J. Food Sci. Technol.*, 2016, **51**(6), 1473–1480.
31 V. K. Pandey, S. N. Upadhyay, K. Niranjan and P. K. Mishra, *Int. J. Biol. Macromol.*, 2020, **157**, 212–219.
32 M. C. Dubey and D. Mohanta, *Phys. Fluids*, 2024, **36**, 017122.
33 S. Hazra and M. Sontakke, *Pharma Innovation*, 2023, **12**(5), 1874–1883.
34 A. Rana, O. Dogiparthi, S. D. Sakhare, B. V. S. Rao and A. A. Inamdar, *J. Food Sci. Technol.*, 2023, **60**(7), 2042–2049.
35 C. Annandarajah, P. Li, M. Michel, Y. Chen, R. Jamshidi, A. Kiziltas, R. Hoch, D. Grewell and R. Montazami, *Materials*, 2018, **12**(1), 99.
36 I. A. Lopes, L. C. Paixao, L. J. S. da Silva, A. A. Rocha, A. K. D. Barros Filho and A. A. Santana, *Carbohydr. Polym.*, 2020, **234**, 115747.
37 U. Plengnok and K. Jarukumjorn, *Biointerface Res. Appl. Chem.*, 2020, **10**(3), 5675–5678.
38 P. Sukyai, P. Anongjanya, N. Bunyahwuthakul, K. Kongsin, N. Harnkarnsujarit, U. Sukatta, R. Sothornvit and R. J. F. R. I. Chollakup, *Food Res. Int.*, 2018, **107**, 528–535.
39 B. H. Patel, P. V. Joshi and J. Packag, *Technol. Res.*, 2020, **4**, 95–101.
40 R. Jagadeesan, I. Suyambulingam, D. Divakaran and S. Siengchin, *Biomass Convers. Biorefin.*, 2023, **13**(5), 4443–4458.
41 J. Wu, X. Du, Z. Yin, S. Xu, S. Xu and Y. Zhang, *Carbohydr. Polym.*, 2019, **211**, 49–56.
42 R. F. Faradilla, G. Lee, J. Roberts, P. Martens, M. Stenzel and J. Arcot, *Cellulose*, 2018, **25**, 399–416.
43 T. G. D. Oliveira, G. L. D. A. Makishi, H. N. M. Chambi, A. M. Q. B. Bittante, R. V. Lourenço and P. J. D. A. Sobral, *Ind. Crops Prod.*, 2015, **67**, 355–363.
44 B. V. Otenda, P. G. Kareru, E. S. Madivoli, E. G. Maina, S. I. Wanakai and W. C. Wanyonyi, *J. Nat. Fibers*, 2022, **19**(10), 3585–3597.
45 J. A. Simão, V. B. Carmona, J. M. Marconcini, L. H. C. Mattoso, S. T. Barsberg and A. R. Sanadi, *Mater. Res.*, 2016, **19**, 746–751.
46 L. Prasad, S. Kumar, R. V. Patel, A. Yadav, V. Kumar and J. Winczek, *Materials*, 2020, **13**(23), 5387.
47 N. Shahi, B. Min, B. Sapkota and V. K. Rangari, *Sustainability*, 2020, **12**(15), 6015.
48 S. S. Kumar and V. M. Raja, *Compos. Sci. Technol.*, 2021, **208**, 108695.
49 A. Divyashree, S. A. B. A. Manaf, S. Yallappa, K. Chaitra, N. Kathyayini and G. Hegde, *J. Energy Chem.*, 2016, **25**(5), 880–887.
50 D. L. Sivadas, A. Damodaran and R. Raghavan, *ACS Sustain. Chem. Eng.*, 2019, **7**(15), 12807–12816.
51 B. Ai, L. Zheng, W. Li, X. Zheng, Y. Yang, D. Xiao, J. Shi and Z. Sheng, *Front. Plant Sci.*, 2021, **12**, 625878.
52 W. G. Abera, R. Kasirajan and S. L. Majamo, *Biomass Convers. Biorefin.*, 2024, **14**(17), 20419–20440.
53 F. S. da Luz, V. S. Candido, A. C. R. da Silva and S. N. Monteiro, *JOM*, 2018, **70**, 1965–1971.
54 K. Sathasivam, M. R. H. Mas Haris and K. Noorsal, *Polym.-Plast. Technol. Eng.*, 2010, **49**(13), 1378–1384.
55 W. N. Gilfillan, L. Moghaddam and W. O. Doherty, *Cellulose*, 2014, **21**, 2695–2712.
56 W. Li, Y. Zhang, J. Li, Y. Zhou, R. Li and W. Zhou, *Carbohydr. Polym.*, 2015, **132**, 513–519.
57 A. R. Ferreira, V. D. Alves and I. M. Coelhoso, *Membranes*, 2016, **6**(2), 22.
58 M. P. Harikrishnan, V. Vishnu, A. Kothakota, R. Pandiselvam, T. Venkatesh, S. Pillai and M. R. Manikantan, *J. Nat. Fibers*, 2023, **20**(1), 2161690.
59 B. Dan-Asabe, S. A. Yaro, D. S. Yawas and S. Y. Aku, *Int. J. Innov. Res. Sci. Eng. Technol.*, 2013, **2**, 5561–5566.
60 N. Lucas, C. Bienaime, C. Belloy, M. Queneudec, F. Silvestre and J. E. Nava-Saucedo, *Chemosphere*, 2008, **73**(4), 429–442.
61 N. H. P. Rodrigues, J. T. de Souza, R. L. Rodrigues, M. H. G. Canteri, S. M. K. Tramontin and A. C. de Francisco, *Appl. Sci.*, 2020, **10**(7), 2235.
62 D. C. Ferreira, G. Molina and F. M. Pelissari, *Composites, Part B*, 2020, **183**, 107682.